Analysis of Magnetic Rollers with the Finite Element Method

Ronny Mertens, Stefan Henneberger, Kay Hameyer and Ronnie Belmans
Katholieke Universiteit Leuven, Dep. EE (ESAT), Div. ELEN, Kardinaal Mercierlaan 94, B-3001 Heverlee, Belgium

***Abstract* - Multipole configurations are used as magnetic rollers in eddy current separators as well as in copy machines. The magnetic field attracts ferromagnetic particles. Therefore, it is the aim to calculate the magnetic field distribution and the force density distribution, even if only the magnetic field outside the magnetic roller is available. Transforming the measured magnetic field values into a set of magnetic vector potentials and using them as the magnetic source in the finite element analysis, makes this method independent of the real excitation (permanent magnets or electromagnets). In this way it is possible to evaluate the force components acting on the particles.**

I. General Computation Method

A. Introduction

For obvious reasons, it is not possible to measure the magnetic flux density inside a multipole magnetic roller. On the other hand the real configuration of the field excitation is not always known. In order to simulate the excitation, the measured values of the normal component of the magnetic flux density $B_n(r_1,\rho)$ at a sleeve of radius r_1 outside the magnetic roller can be transformed into a set of magnetic vector potentials. This set can be used as the magnetic source in the finite element analysis. Fig. 1 shows the distribution of the magnetic field for an arbitrary 4-pole configuration.

B. First order elements

The transformation is based on the solution of Laplace's equation in circular co-ordinates and the boundary condition $\boldsymbol{A}(\infty,\rho) = 0$. In the two-dimensional case the magnetic vector potential $\boldsymbol{A}$ has only a value in the z-direction. The general solution for the magnetic vector potential $A(r,\rho)$ in the z-direction is given by the Fourier series [2]

$$A(r,\rho) = \sum_{k=1}^{N}\left(A_{k,1}\left(\frac{r_1}{r}\right)^k \cos(k\rho) + A_{k,2}\left(\frac{r_1}{r}\right)^k \sin(k\rho)\right). \qquad (1)$$

Manuscript received July 10, 1995.

R. Mertens, e-mail Ronny.Mertens@esat.kuleuven.ac.be; St. Henneberger, e-mail Stefan.Henneberger@esat.kuleuven.ac.be; K. Hameyer, e-mail Kay.Hameyer@esat.kuleuven.ac.be; R. Belmans, e-mail Ronnie.Belmans@ esat.kuleuven.ac.be; phone +32 16 32 10 20, fax +32 16 32 19 85.

The authors are grateful to Agfa Gevaert N.V., especially to ir. R. Janssens, Dr. Sc. D. Broddin and Mr. L. Van Goethem for their support and for performing the measurements, and to the Belgium Ministry of Scientific Research for granting the IUAP No. 51 on Magnetic Fields and the Council of the Belgian National Science Foundation.

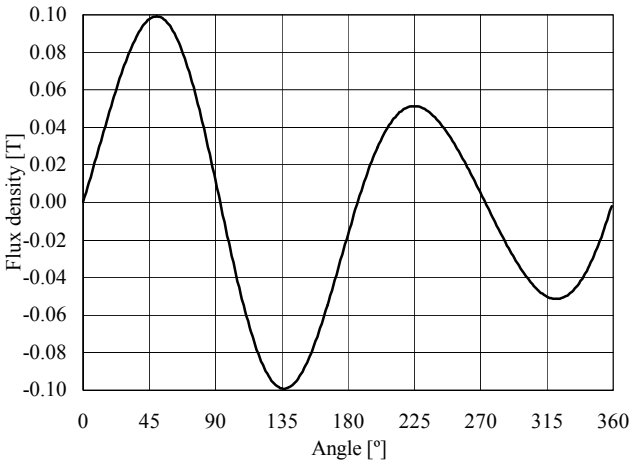

Fig. 1. Normal component of the magnetic flux density $B_n(r_1,\rho)$ derived from measurements.

With curl $\boldsymbol{A} = \boldsymbol{B}$, the normal component $B_n(r,\rho)$ and the tangential component $B_t(r,\rho)$ of the flux density are given by

$$B_n(r,\rho) = \sum_{k=1}^{N}\left(k\,A_{k,2}\frac{r_1^k}{r^{k+1}}\cos(k\rho) - k\,A_{k,1}\frac{r_1^k}{r^{k+1}}\sin(k\rho)\right) \qquad (2)$$

and

$$B_t(r,\rho) = \sum_{k=1}^{N}\left(k\,A_{k,1}\frac{r_1^k}{r^{k+1}}\cos(k\rho) + k\,A_{k,2}\frac{r_1^k}{r^{k+1}}\sin(k\rho)\right). \qquad (3)$$

Due to the discretisation errors of the finite element analysis, this solution $A(r,\rho)$ (1) is valid for a radius $r \geq r_1 + \Delta r$. To avoid this limitations one can transform the

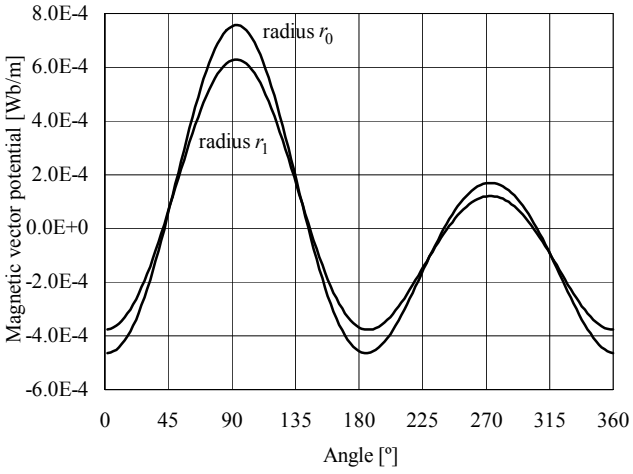

Fig. 2. Computed magnetic vector potential $A(r_1,\rho)$ and $A(r_0,\rho)$.

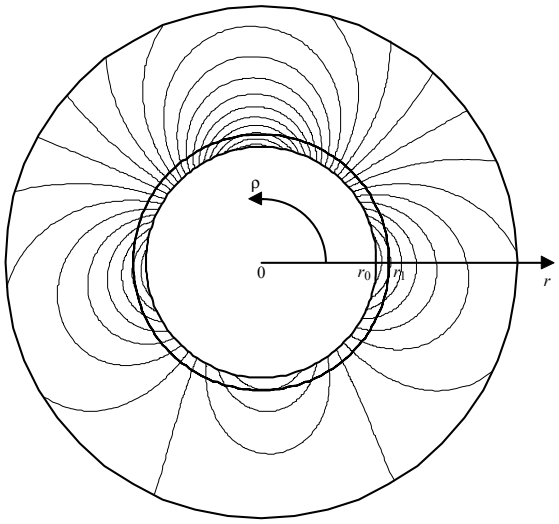

Fig. 3. Flux plot of the arbitrary 4-pole configuration.

set of magnetic vector potentials into another set at a radius r_0 inside the magnetic roller with $0 \le r_0 \le r_1$ and giving the same flux density at the radius r_1. This means that the solution $A(r,\rho)$ is valid for an arbitrary radius outside the magnetic roller. Fig. 2. shows the vector potential $A(r_1,\rho)$ at a radius r_1 and $A(r_0,\rho)$ at a radius r_0 inside the magnetic roller. The approximation with 180 values of the magnetic vector potential and using the open boundary technique [3] results in the flux plot of Fig. 3.

The field distribution (2) compared with the results obtained with the method mentioned leads to a small error. The error e is defined by

$$e = \left| \frac{\max\left(B_{FEM}(r_1,\rho)\right) - \max\left(B_n(r_1,\rho)\right)}{\max\left(B_n(r_1,\rho)\right)} \right|, \tag{4}$$

where $B_{FEM}(r_1,\rho)$ is the normal component of the magnetic flux density along a circular contour with radius r_1. The error e is lower than 0.1% for each peak value plotted in Fig. 1.

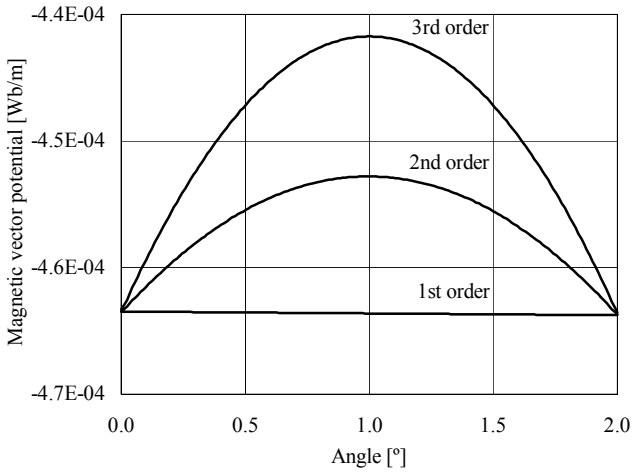

Fig. 4. Magnetic vector potential along the edge of an element.

C. Higher order elements

To achieve the same accuracy, an iterative method is necessary for higher order elements. Fig. 4 shows the magnetic vector potential along the edge of an element at the inner boundary of the finite element model. Because 180 values are used for the magnetic source, this edge corresponds with an angle of 2°. The first order approximation coincides with the general solution (1). Due to the difference in contents of circular harmonics, the values of the magnetic vector potential used as the magnetic source at radius r_0, are adapted to obtain the desired flux density at the radius r_1. Two or three iterative steps are usually sufficient to obtain the same accuracy.

II. Force Calculation

The force is calculated by using the change of the stored magnetic energy. The magnetic energy density is

$$w_{mag} = \frac{B \cdot H}{2} = \frac{\mu H^2}{2}. \tag{5}$$

If air is replaced by magnetic material with a relative permeability μ_r, the energy difference is

$$\Delta w_{mag} = \frac{\mu_0 \mu_r H^2}{2} - \frac{\mu_0 H^2}{2}. \tag{6}$$

The force density is obtained by the derivative of Δw_{mag}:

$$f = \frac{\mathrm{d}F}{\mathrm{d}V} = \mu_0(\mu_r - 1)\,\mathrm{grad}\,H^2. \tag{7}$$

An equivalent formulation for the magnetic force density can be found in [6]. Fig. 5 shows the force density for the arbitrary 4-pole configuration along a circular contour at a distance of 1 mm from the sleeve. The sleeve has a radius of 10 mm. The particles of the magnetic powder have a low relative permeability $\mu_r = 10$.

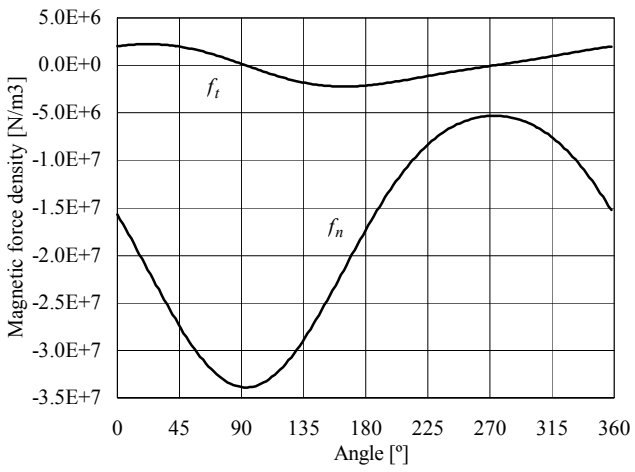

Fig. 5. Magnetic force density $f(r_1 + 1\ \mathrm{mm},\rho)$.

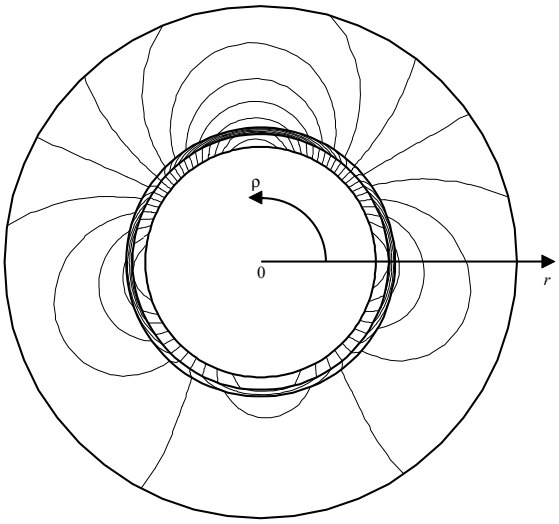

Fig. 6. Flux plot of the arbitrary 4-pole magnetic roller covered with a skin of magnetic powder.

III. Multi-Skin Approach

The multi-skin approach is an extension of the same technique. This is the case when the magnetic powder forms a skin around the magnetic roller or when materials with a different relative permeability are used. It is assumed that the skin is approximated as uniformly thick. The outer skin is formed by the surrounding air.

The full formulation for the magnetic vector potential in the inner skins has to be used:

$$A(r,\rho)=\sum_{k=1}^{N}\left(A_{k,1}\left(\frac{r_1}{r}\right)^k\cos(k\rho)+A_{k,2}\left(\frac{r_1}{r}\right)^k\sin(k\rho)+A_{k,3}\left(\frac{r}{r_1}\right)^k\cos(k\rho)+A_{k,4}\left(\frac{r}{r_1}\right)^k\sin(k\rho)\right). \quad (8)$$

For the surrounding air the formulation of (1) can still be used. All the coefficients for the different formulation in each skin are determined by the boundary conditions. At the boundary of radius r_1 between skin 1 and skin 2 yields

$$B_{n,1}(r_1,\rho)=B_{n,2}(r_1,\rho) \quad (9)$$

and

$$H_{t,1}(r_1,\rho)=H_{t,2}(r_1,\rho)\Leftrightarrow\frac{B_{t,1}(r_1,\rho)}{\mu_1}=\frac{B_{t,2}(r_1,\rho)}{\mu_2}. \quad (10)$$

Skin 1 is formed by the sleeve and skin 2 by the magnetic powder. The same boundary conditions are valid for the boundary between skin 2 and 3. This results in a set of equations for each circular harmonic.

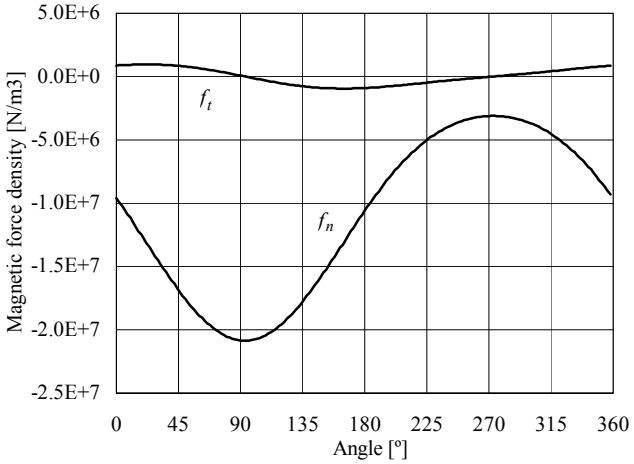

Fig. 7. Magnetic force density $f(r_1 + 1\text{ mm},\rho)$.

Fig. 6 shows the flux plot of the same arbitrary 4-pole magnetic roller, which means that the same values for the magnetic vector potential are used as magnetic source. The magnetic powder forms a skin of thickness 0.5 mm. Fig. 7 shows the force density along a circular contour at a distance of 1 mm from the sleeve. The magnetic powder acts as a magnetic shield around the magnetic roller.

IV. Conclusion

The method of transforming measured magnetic flux density values into a set of magnetic vector potentials, can be used to examine the behaviour of magnetic particles in the neighbourhood of a magnetic roller. In order to calculate the distribution of the force density, it is not required to have any information about the interior of the magnetic roller.

References

[1] Masao Nakano, Toshinori Ando and Kazuhisa Kemmochi, “Analysis of Toner Motion in the Development Process,” *9th International Congress on Advances in Non-Impact Printing Technologies*, October 4 - 8, 1993.

[2] K. J. Binns, P. J. Lawrenson and C. W. Trowbridge, *The analytical and numerical solution of electric and magnetic fields*, John Wiley & Sons, 1992.

[3] D. A. Lowther and E. M. Freeman, "Further aspects of the Kelvin transformation method for dealing with open boundaries," *IEEE Trans. on Magnetics*, Vol. 28, No. 2, pp. 1667 - 1670, March 1992.

[4] Wen-Ling Fang and Der-Ray Huang, “Analysis of a quadruple bonded Nd-Fe-B magnetic roller,” *Journal of Applied Physics*, Vol. 70, No. 10 pt. 2, pp. 6618 - 6620, November 1991.

[5] P. P. Silvester and R. L. Ferrari, *Finite elements for Electrical Engineers*, Cambridge University Press, 1990.

[6] T. B. Jones, G. L. Whittaker and T. J. Sulenski, “Mechanics of magnetic powders,” *Powder Technology*, No. 49, pp. 149-164, 1987.